

## **PROBING THE SMALL-SIZE DEBRIS ENVIRONMENT IN THE GEOSTATIONARY RING**

**T. Schildknecht<sup>(1)</sup>, R. Musci<sup>(1)</sup>, M. Ploner<sup>(1)</sup>, W. Flury<sup>(2)</sup>, J. Kuusela<sup>(3)</sup>, J. de Leon Cruz<sup>(4)</sup>,  
L. de Fatima Dominguez Palmero<sup>(4)</sup>**

<sup>(1)</sup> *Astronomical Institute, University of Bern, Sidlerstrasse 5, CH-3012 Bern, Switzerland*  
*Email: thomas.schildknecht@aiub.unibe.ch*  
*Email: reto.musci@aiub.unibe.ch*  
*Email: martin.ploner@aiub.unibe.ch*

<sup>(2)</sup> *ESA ESOC, Robert-Bosch-Strasse 5, 64293 Darmstadt, Germany*  
*Email: Walter.Flury@esa.int*

<sup>(3)</sup> *ASRO, Turku, Finland*  
*Email: jyri.kuusela@asro-space.com*

<sup>(4)</sup> *Instituto de Astrofisica de Canarias, 38200 La Laguna, Tenerife, España*  
*Email: jmlc@ot.iac.es*  
*Email: ldp@ll.iac.es*

### **ABSTRACT**

The space debris population in low Earth orbits (LEO) has been extensively studied during the last decade and reasonable models covering all size ranges were produced. Information on the distribution of objects in the geostationary ring (GEO), however, is still comparatively sparse. Until recently the population of man-made objects in GEO had to be inferred solely from the about 900 continuously tracked objects and the modeling of the two explosions known to have occurred in GEO.

Optical observations from the last two years performed with ESA's 1-meter telescope at the Teide observatory in Tenerife changed the situation substantially. A hitherto unknown but significant population of small-size objects with diameters as small as 10 centimeters has been detected. The current survey technique yields statistical orbit information, but must assume circular orbits for all objects.

The paper will summarize recent results from the ESA GEO surveys and outline a technique to estimate eccentricities at discovery time by combining observations taken quasi-simultaneously from different observation sites.

### **1. INTRODUCTION**

The space debris population in low Earth orbits (LEO) has been extensively studied during the last decade and reasonable models covering all size ranges were produced. Information on the distribution of objects in the geostationary ring (GEO), however, is still comparatively sparse. The safety requirements for manned space flight, especially for the international space station ISS, were a main concern, and consequently research focussed on the debris environment in LEO. Moreover the vast majority of the more than 150 known explosions in space took place in LEO or in eccentric orbits crossing the LEO region. Explosive events are responsible for more than 40% of the population of objects larger than about 20cm, i.e. of the USSPACECOM catalogue population in LEO. Debris in the 1-10cm size range, although too small to be tracked by operational USSPACECOM systems, is still large enough to cause catastrophic damage to most satellites. Thousands of particles of this size must have been produced by many of the mentioned explosions. Radar, optical and in situ measurements, in combination with explosion models, allowed developing reliable debris population models for LEO covering the size range from microns to meters.

For GEO our knowledge is comparatively poor. The larger distances limit the object sizes to be sensed by most operational optical and Radar systems to about one meter – roughly the estimated limiting size of the USSPACECOM catalogue. Only two explosions are known to have occurred in GEO (a breakup of an Ekran spacecraft in 1978 and an explosion of a Titan rocket upper stage in 1992). Current models for GEO are either based on the catalogue population only, or they add fragments from the two explosions to the catalogue population. In both cases the models end up with a much lower spatial density of small objects in the GEO region than in most LEO altitudes. This result has in turn sometimes be used as an argument to focus on the (apparently) much denser and thus more critical LEO environment.

However, given the fact that we were mostly ‘blind’ for GEO objects smaller than one meter in the past, the models might rather reflect the missing input from observations than the real GEO environment. The Inter-Agency Space Debris Coordination Committee (IADC), an international governmental forum including all major space fairing nations, recognized this deficiency. The IADC initiated a first international campaign to optically survey the GEO region in 1995, followed by a second campaign in 2002. The objectives of these campaigns were to collect information on the extent and character of the GEO debris population, specifically by obtaining statistical distributions of the brightness and of the orbital elements.

Subsequently several organizations started optical surveys of the GEO region. The European Space Agency ESA, in particular, was setting up an optical debris survey system using its 1-meter telescope on Tenerife, Canary Islands. This system is operational since 1999. It has been used for several GEO surveys and contributed substantially to both IADC campaigns.

This paper describes the second IADC campaign and compares the ESA data of this survey with results from other ESA campaigns. We will focus on the ‘orbit determination problem’ and the associated problem of interpreting the resulting distributions of orbital elements. A possible remedy using simultaneous observations from different sites will be presented. The feasibility of the method will be illustrated with the results from a trial campaign.

## 2. PLANNING OF THE SPRING 2002 IADC CAMPAIGN

At the time of the first IADC GEO campaign there seemed to be no need for a common observation plan and the surveys took the form of individual campaigns. The results from the individual surveys did not agree with each other but the differences could be attributed to observational biases [1]. As a consequence it was decided to use a common observation plan for the second IADC campaign in order to produce, although not bias free, but at least comparable results.

Debris released from objects in GEO, e.g. mission related objects or material released due to aging processes, is expected to stay in orbits similar to the orbits of their parent bodies. Even pieces stemming from explosions in GEO will generally remain in the GEO region. The energy increment or decrement they get during the explosion is usually not sufficient to considerably alter their orbital plane or their semimajor axis. The debris will not only start with orbits similar to their parent objects, but their orbits will also undergo similar perturbations and thus evolve in a similar way (the latter may not be true for objects with a very large area to mass ration which react differently to radiation pressure forces). It is therefore reasonable to assume the simple hypothesis that the catalogued GEO objects trace the debris population. It is obvious that the detailed orbital characteristics of these two populations will certainly differ from each other (we expect debris from distinct explosion events) but in general we expect them to occupy the same region in the orbital element space.

Fig. 1 shows the apparent density of the catalogued GEO objects (gray shaded area) in the right ascension-declination-space as seen from the geocenter. The sinusoidal pattern is due to a specific distribution of the orbital planes, which in turn is due to gravitational perturbations. The orbital planes of uncontrolled objects in GEO exhibit precessional motions, which manifests themselves in periodic variations of the inclinations between 0 and 15 degrees with a period of about 53 years. These precessional motions also result in a correlation between the inclinations and the right ascensions of the ascending nodes. This is best seen in a polar diagram as given in Fig. 2.

When defining the search fields there is a series of observational constraints to be taken into account. First of all the objects should be observed under good illumination conditions (the so-called phase angle should be small), which means that the best locations are near the Earth shadow cone (but still outside the shadow region!). Dense stellar background regions, in particular the Milky Way, must be avoided. The fields should be at high elevations for a good part of the night; the angular distance from the moon should be maximized, etc. Last but not least the field should cover the dense region of the catalogue population where we expect – according to the mentioned hypothesis – the most debris pieces. The fields of the 2002 spring IADC campaign shown in Fig. 1 satisfy these criteria. We defined one field for each night to be observed by all participating stations as long as possible during this particular night. The centers of the IADC search fields are defined as geocentric positions but they should be transformed to

topocentric positions (i.e. the parallax should be applied) so that each observatory is actually sampling the same region in GEO.

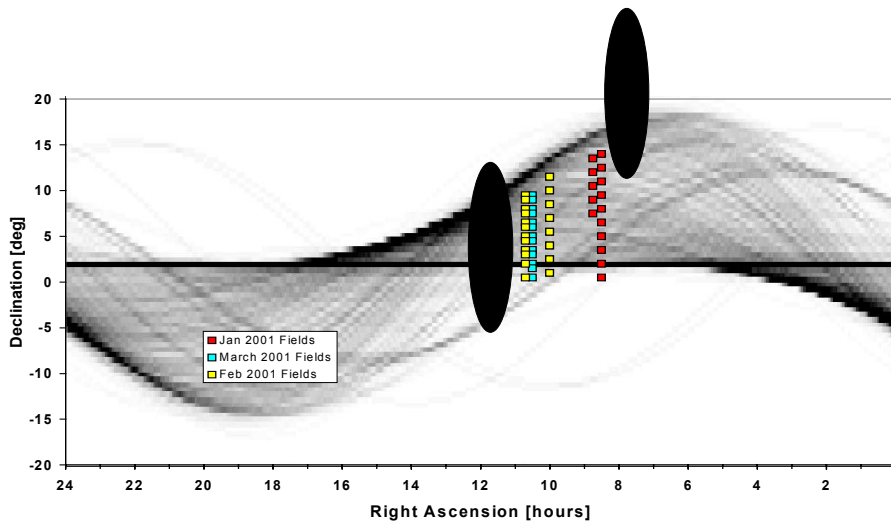


Fig. 1. Apparent density of the catalogued GEO objects in the right ascension-declination-space. The small squares mark survey fields of the IADC 2002 GEO survey campaign. The dark ellipses indicates the Earth shadow on January 15 and March 15. (Some of the March fields are hidden behind the February fields.)

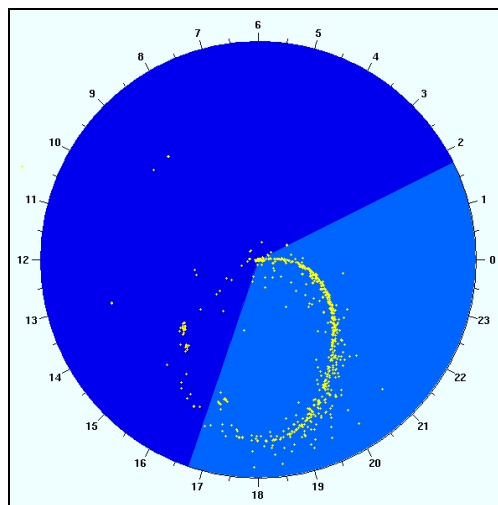


Fig. 2. Polar diagram (right ascension, declination) showing the orbital poles of the catalogued GEO objects.

### 3. ESA OBSERVATIONS

#### 3.1. The ESA Space Debris Telescope

Fig. 3 shows the dome of the ESA Space Debris Telescope at the Teide Observatory on Tenerife, Canary Islands. The observatory is located at 2400 meters above seal level, about 20km from the Teide volcano. The site is known for its excellent seeing, but light pollution from the densely populated coastal areas of the island prevents the optimum use of large telescopes. The ESA Space Debris Telescope is a classical astronomical telescope with a 1-meter primary mirror and an English mount. For the debris observations we use the modified Richey-Crétien focus which is equipped with a CCD camera. The focal plane array consists of a mosaic of four 2k x 2k pixel CCDs. The total field of view is about 0.7 x 0.7 square degrees and the pixel size is 0.6 arcseconds.



Fig. 3. Dome of the ESA Space Debris Observation Telescope at the Teide Observatory on Tenerife, Canary Islands. The Teide volcano seen in the background is the highest peak of Spain (3,715 m) and the third largest volcano on Earth (after Mauna Loa and Mauna Kea).

### **3.2. The Survey Technique**

The detection technique is based on an algorithm comparing several consecutive frames of the same field in the sky. Background stars are identified on a series of 10 to 30 frames, and the remaining parts of the frames are scanned for any additional objects. During the exposures the telescope is staring into an Earth fixed direction, i.e. it is not tracking the stars but potential geostationary objects. After each exposure the telescope has to be repositioned so that the same area of the sky is passing the field of view at the next exposure. The frames are usually exposed for 2 seconds, which is a compromise between a high signal to noise ratio for the objects (long exposures) and a reasonable length for the star trails (short exposure). The exposure repetition rate for a particular field was set to one per minute meaning that any geosynchronous object detected would be visible on three consecutive frames. Given the current maximum frame repetition rate of about one per 30 seconds (including the repositioning of the telescope) we are able to observe two adjacent fields in parallel.

One ‘observation unit’ usually consists of a series of 60 exposures of the same celestial field and lasts about 30 minutes. The geocentric IADC field coordinates were separately transformed to topocentric coordinates for each observation unit. I.e. the parallax was not applied for each exposure – our detection technique needs a series of frames of the same celestial field – but once per 30-minute batch. These batches are then processed in quasi-real-time at the observatory and the results are available about 30 minutes after the observation.

### **3.3. Results**

ESA has been conducting several GEO survey campaigns during the past years. Table 1 gives an overview of the ESA GEO campaigns until March 2002. The table includes the 1999 test campaign, which consisted in fact of a first, very limited series of system tests. But nevertheless the data from this campaign significantly contributed to the results of the first IADC GEO survey campaign [1]. The terms ‘correlated object’ and ‘uncorrelated object’ refer to objects which correlate or do not correlate with the catalogue. We used the unclassified part of the USSPACECOM catalogue as our reference. By ‘uncorrelated detection’ we denote the detection of an uncorrelated object within a single 30-minute observation series. Some of these detections may actually refer to the same object, i.e. we may have incidentally re-observed some of the objects during the campaign. We use the term ‘uncorrelated objects’ for uncorrelated objects after having correlated all detections from the campaign. This latter task is identical with the creation and maintenance of a temporary catalogue of orbital elements for the unknown objects and has been performed for the first campaign only.

Table 1. ESA GEO Campaigns

	Aug/Sept 1999 (1 <sup>st</sup> IADC Campaign)	Jan – Jul 2001	Jan – Mar 2002 (2 <sup>nd</sup> IADC Campaign)
Frames	5'400	62'500	30'100
Scanned Area	895 deg <sup>2</sup>	11200 deg <sup>2</sup>	4280 deg <sup>2</sup>
Obs. Time	13 nights / 49 h	82 nights / 521 h	30 nights / 251 h
Image Data	52 GB	500 GB	140 GB
Correlated detections	180	2'023	557
Correlated objects	56	448	252
<b>Uncorrelated detections</b>	<b>348</b>	<b>1'587</b>	<b>779</b>
<b>Uncorrelated objects</b>	<b>150</b>	<b>?</b>	<b>?</b>

At this point it is very important to draw our attention again to the fact that all surveys in Table 1 suffer from observational biases. Or in other words ‘what we see depends on where and when we look’. The numbers given in Table 1 could therefore be misleading, e.g. when simply taking the ratio of uncorrelated to correlated detections as a measure to estimate the total number of debris objects!

#### Absolute Magnitude Distribution

Fig. 4 shows the absolute magnitude distribution of all detections from the IADC January to April 2002 campaign. The corresponding Figure for the data set of the January to July 2001 campaign is given in Fig. 5. The solid lines indicate the instrument sensitivity as determined from independent calibration measurements. All magnitudes have been reduced from apparent magnitudes to so-called absolute magnitudes by correcting for the illumination phase angle. For the scattering properties we assumed a simple Lambertian sphere. No reduction to a common distance has been done because of the uncertainties of the determined orbits (see below). The value of this correction would be less than 0.5 magnitudes in most cases. The magnitudes are astronomical ‘V magnitudes’ and have an accuracy of a few 0.1 magnitudes except for the very faint objects where errors could amount to 0.5 – 1 magnitude. The indicated object sizes were derived by assuming Lambertian spheres and a Bond albedo of 0.1. Both assumptions, however, are uncertain, as long as we don’t know the nature of the observed objects.

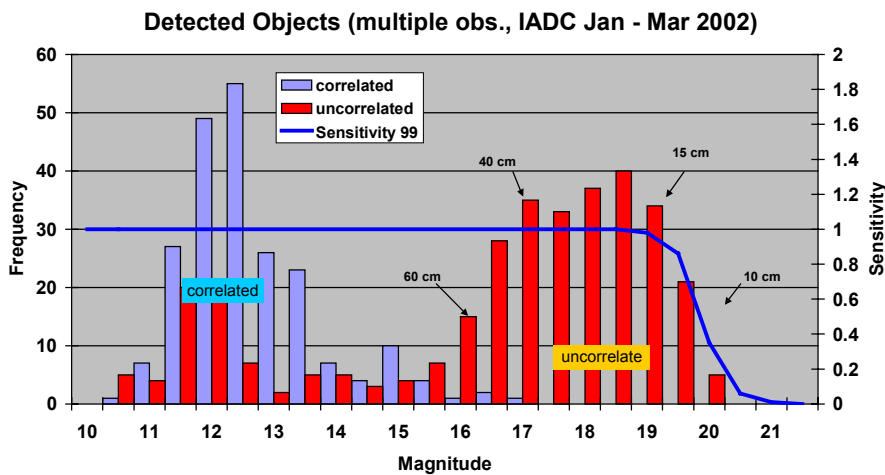


Fig. 4. Absolute magnitude distribution for the detections of the IADC January to March 2002 campaign.

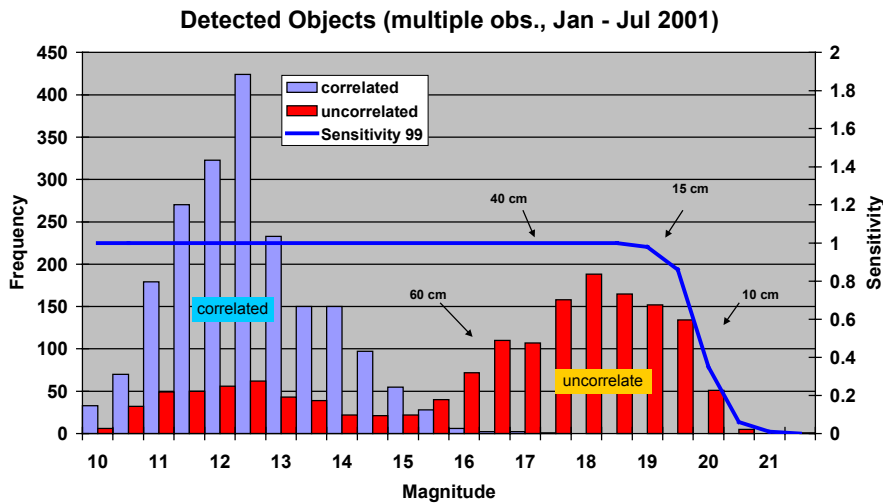


Fig. 5. Absolute magnitude distribution for the detections of the January to July 2001 campaign.

The distribution is bimodal for both campaigns. The distribution of the correlated objects has its peak at about magnitude 12.5 and spreads from about magnitude 10 to 15. It is also slightly asymmetric with the slope on the fainter end being shallower. This distribution nicely reflects the size distribution in the catalogue. The uncorrelated objects seem to be concentrated in a broad strong peak around magnitude 18 to 18.5 and in a second much less pronounced peak which follows more or less the distribution of correlated objects.

The bright objects in the latter peak are most likely all ‘known’, large objects, which did not correlate with the catalogue for several reasons. Some of these objects are classified and were therefore not included in the ‘unclassified’ version of the catalogue. Others might well be in the catalogue but did not correlate due to insufficient accuracy of the catalogue. In many cases these objects are members of groups of satellites co-located in the same 0.1-degree longitude slot. They often correlate with several objects in the catalogue, again due to the limited accuracy of the catalogue, and thus end up as ‘uncorrelated’ due to confusion. Finally the catalogue might be incomplete at the fainter end.

The uncorrelated objects in the range from magnitude 15 to 21 are smaller than the minimum size of the objects in the catalogue. The apparent main peak of this population at about magnitude 18 is in fact not a peak, because the cutoff in number of objects fainter than about magnitude 19 is entirely due to the sensitivity limit of the observation system (see the line indicating system sensitivity). The real luminosity function beyond magnitude 19 could therefore still increase!

The IADC campaign nicely confirms the result from the much longer ESA campaign in 2001. Although the detailed structure of the distributions differ due to observation biases (the survey fields were different, and the 2001 ESA campaign comprises much more data) the overall characteristics and especially the locations of the peaks match perfectly.

### Inclination Distribution

The inclination distributions for the IADC January to April 2002 and the January to July 2001 campaigns are shown in Fig. 6 and Fig. 7, respectively. The distribution of the uncorrelated detections roughly follows the distribution of the correlated detections for inclinations lower than about 11 degrees in both campaigns. For higher inclinations there is a clear excess of uncorrelated detections. In the January to July 2001 campaign (Fig. 7) there are even two distinct concentrations of uncorelated objects around 13 and 15 degree inclination.

### Distribution of Semimajor Axes

Fig. 8 and Fig. 9 show the distributions of the semimajor axes of both campaigns. Again, the distributions are very similar. Both, the correlated and the uncorrelated objects, are concentrated around the nominal GEO altitude. The semimajor axes of the uncorrelated objects, however, are much more dispersed showing a significant asymmetry with an excess at large values.

Its is important to mention that all semimajor axes were determined assuming circular orbits, which is certainly not true for all objects. In general, fixing the eccentricity at a wrong value may result in a large error of the inferred semimajor axis. Part of the spread for the uncorrelated objects, as well as some of the large values may be due to this

effect. Objects on highly elliptic orbits having their apogee near GEO may mimic objects in much higher circular orbits when observed at apogee. This is in particular the case for objects on a geostationary transfer orbit (GTO). Fitting circular orbits through observations of GTOs near their apogee yields semimajor axes of the order of 50000 kilometers whereas the real values would be about 26000 kilometers but with an eccentricity of 0.73 instead of 0.

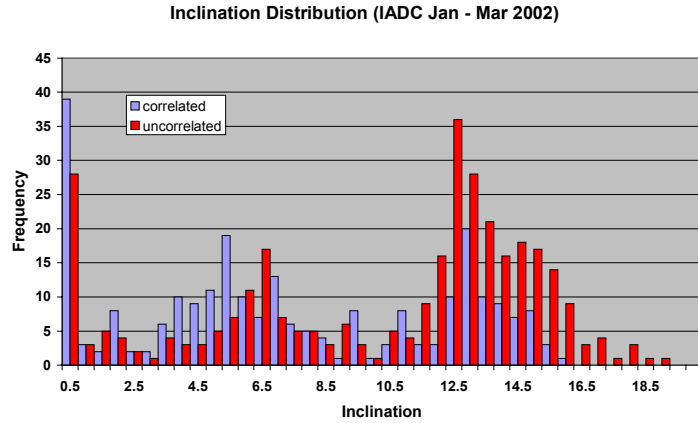


Fig. 6. Inclination distribution for detections of the IADC January to March 2002 campaign.

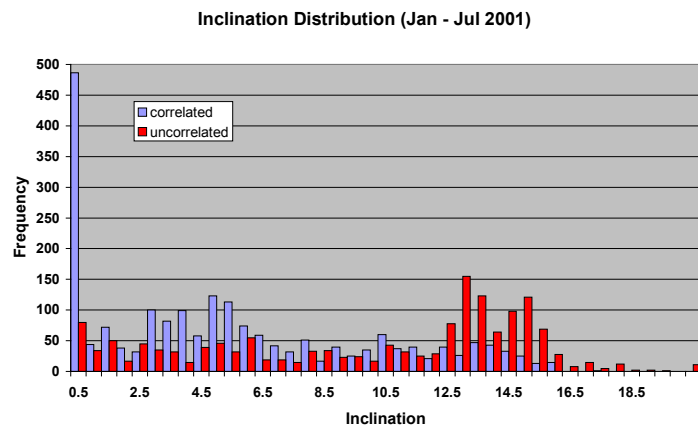


Fig. 7. Inclination distribution for detections of the January to July 2001 campaign.

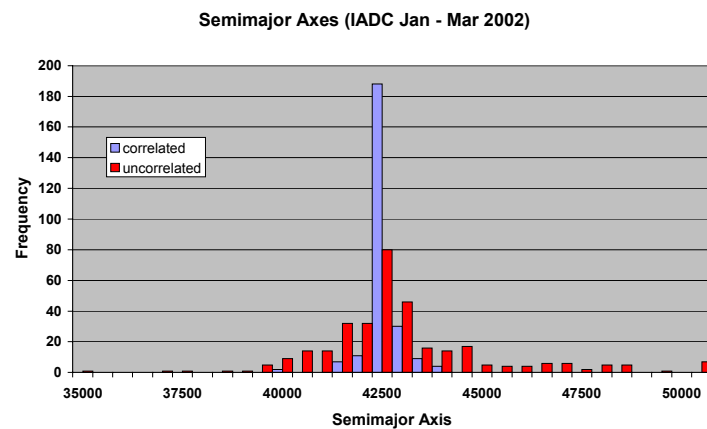


Fig. 8. Distribution Semimajor axes for detections of the IADC January to March 2002 campaign.

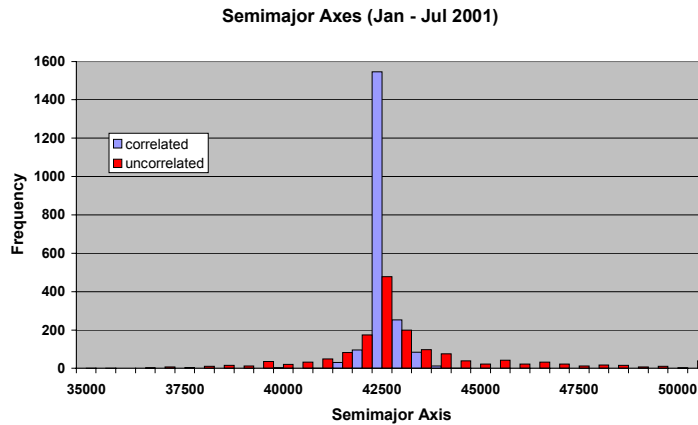


Fig. 9. Distribution Semimajor axes for detections of the January to July 2001 campaign.

### Orbit Inclination and Right Ascension of Ascending Node

The inclinations and right ascensions of the ascending nodes are strongly correlated for the TLE population as we have seen in section 2. Fig. 10 and Fig. 11 give both elements for all correlated and uncorrelated detections of the IADC 2002 and the ESA 2001 campaign respectively. The distinct figure outlined by the correlated objects is due to the explained 53-year precession period of the orbital planes. Assuming that the objects started with orbits of 0 degree inclination the position in the diagram is indicating the time since the end of active inclination control. The orbits gradually evolve from low inclination and at right ascension of the ascending node of about 100 degrees to higher inclinations and lower right ascension of the node until they reach the maximum inclination of 15 degrees after 26.5 years. The oldest catalogue objects have already passed this point.

The correlated objects of both campaigns (left diagrams of Fig. 10 and Fig. 11) nicely show this evolutionary pattern. With a few exceptions the controlled satellites can be found at 0 degree inclination ( $I$ ) at all right ascensions for their ascending nodes (RAAN). Uncontrolled objects lie predominantly on the line from  $RAAN \approx 100 / I \approx 0$  to  $RAAN \approx 10 / I \approx 15$ . The latter point is the location where the objects reach the maximum value for the inclination about 26.5 years after the end of active inclination control. A few objects already passed this point and are now in the RAAN interval from  $-40$  to  $100$  degrees at inclinations between  $10$  to  $15$  degrees.

There are only a few uncorrelated objects (right diagrams of Fig. 10 and Fig. 11) residing in the ‘controlled region’ at 0 degree inclination. The bulk of the uncorrelated objects lies again on the mentioned evolution track but with a much larger spread. In addition there is a ‘background’ component with a homogeneous distribution in the  $I/RAAN$  space especially noticeable in the right diagram of Fig. 11. The most striking features in both campaigns, however, are the distinct clusters of objects. Prominent concentrations are found in Fig. 11 at  $RAAN \approx 20 / I \approx 13$ ,  $RAAN \approx 15 / I \approx 14.5$ ,  $RAAN \approx 10 / I \approx 15$  (all with an elliptical shape), and at  $RAAN \approx 50 / I \approx 8$  and  $RAAN \approx -12 / I \approx 12.5$  (both ‘banana-shaped’). There are much less observations from the IADC 2002 campaign compared to the ESA 2001 campaign but the concentrations seen in Fig. 10 all confirm clusters found in the ESA 2001 campaign (Fig. 11)!

We have checked some of the clusters for multiple sightings of the same objects and conclude that they are real (a pure selection effect can be excluded). The only reasonable explanation for the origin of these clusters are explosive events. First attempts to reproduce these results by modeling a series of explosions have been performed (see e.g. [4]). However, still more data will be needed to understand the details of the mechanism or to even trace the clusters back to their parent objects.

The explanation for the ‘background’ component is more difficult. At this time we can not decide if this component is real or an artifact due to the assumed circular orbits. As explained in the paragraph on the inclination distribution, objects on highly elliptic orbits like GTOs may affect the results and could at least partly be responsible for the ‘background’ component.

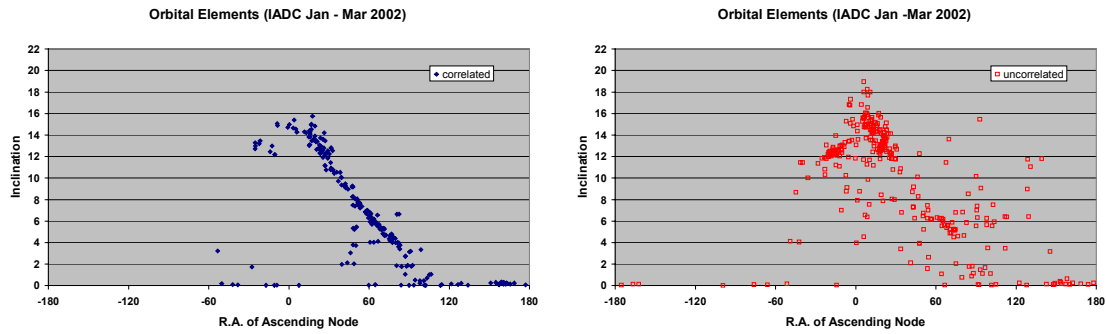


Fig. 10. Inclination versus right ascension of ascending node for the correlated (left) and uncorrelated (right) detections of the IADC January to March 2002 campaign.

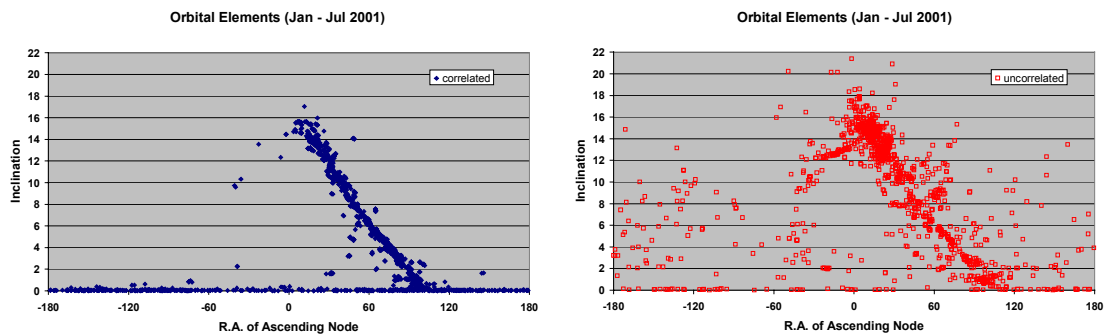


Fig. 11. Inclination versus right ascension of ascending node for the correlated (left) and uncorrelated (right) detections of the January to July 2001 campaign.

#### 4. ORBIT DETERMINATION

Optical surveys are inherently designed such that the objects are detected on a short series of a few frames. The total time interval of these series is of the order of a few minutes. In the case of the Tenerife surveys we observe the objects for about one to two minutes corresponding to two to three frames. These short arcs of angle-only data force us to determine circular orbits. (In principle we could fix any two of the 6 orbital parameters but it is most reasonable to assume circular orbits in GEO.) This lack of eccentricity information will obviously cause errors in the estimation of the remaining orbital elements. The proliferation of erroneous elements will prevent the correlation of detections over a survey campaign, i.e. it will prevent the transition from detections to objects. For objects with considerably eccentric orbits like GTOs there is an even more severe consequence in the context of statistical surveys. The errors of the inferred orbital elements may be so large that the results for these objects mimic a dynamically totally different population compared to the real one (see also the discussion in the previous section).

There are two ways to tackle this problem: we may either try to observe longer arcs or use quasi-simultaneous multi-site observations. The former needs immediate follow-up observations (also called ‘target tracking’) after the discovery. This is very demanding from the point of view of system capabilities, especially in terms of real-time software, and it consumes a considerable amount of the survey time. The latter requires a minimum amount of coordination between different survey sites and, of course, a common observation volume accessible by the participating stations. Processing of the data can be done off-line and we benefit from an independent confirmation of the detections.

The following results stem from a trial study on a short baseline and should illustrate the concept. The Study was jointly initiated by James S.B. Dick from Observatory Sciences Ltd., UK, and one of us (T. Schildknecht) [3]. We used simultaneous observations of the geostationary satellite 98035A from the 1-meter telescope at the Zimmerwald observatory near Bern, Switzerland and from a 0.4-meter PIMS telescope in Gibraltar (1600-kilometer baseline). The so-called PIMS system in Gibraltar is operated by the Observatory Sciences Ltd. UK under contract from the UK Ministry of Defense.

Fig. 12 shows the post-fit residuals (6-parameter orbit determination) for a single-site 15-minute arc of observations from Zimmerwald (left) and for an 8-minute arc from Gibraltar (right). The corresponding values for the estimated semimajor axis ( $a$ ), the eccentricity ( $e$ ), the inclination ( $i$ ) and their formal errors are given in Table 2 (case 1 and case 2). These two cases should primarily illustrate the quality of the measurements and give an impression of the formal errors to be expected for a GEO orbit determined from a 10-minute arc.

For the next test case we used three observations from Gibraltar, all spaced by 25 seconds with a total arc length of 50 seconds. This corresponds to a typical discovery observation series from a survey. From these observations we would usually estimate a circular orbit but for test purposes we tried a 6-parameter orbit determination. The result given in Table 2 (case 3) is clearly indicating that the eccentricity and the inclinations could not be reasonably determined (in most cases the determination process would even become singular).

Finally we combined observations from both sites by adding 3 observations from Zimmerwald mimicking the discovery of the same object on two sites within a time interval of 15 minutes. The temporal spacing of the observations and the residuals can be found in Fig. 13. The eccentricity and the inclination can now be determined reliably (Table 2, case 4). The error of the semimajor axis is significantly smaller than in all other cases, the errors of the remaining elements are smaller than for the 8-minute arc of Gibraltar observations alone (case 2). The results clearly illustrate the benefit of multi-site observations. The gain in accuracy of the determined orbit would be even more significant on longer, e.g. intercontinental baselines.

There were no observations of GTO objects acquired during this test. Although we do not expect any problems with the extension of the method to GTOs, a corresponding campaign should be conducted in near future in order to demonstrate the feasibility.

Table 2. Orbital elements and corresponding errors for several test cases

<i>Case 1</i> – Zimmerwald – 15-minute arc	$a = 42659.5 \pm 251.6 \text{ km}$ $e = 0.0084 \pm 0.0044$ $i = 0.0710 \pm 0.0101 \text{ deg}$ RMS = 0.14 arcs
<i>Case 2</i> – Gibraltar – 8-minute arc	$a = 44446.8 \pm 9333.8 \text{ km}$ $e = 0.0394 \pm 0.1516$ $i = 0.1318 \pm 0.2690 \text{ deg}$ RMS = 1.25 arcs
<i>Case 3</i> – Gibraltar – 3 observations – 50-second arc	$a = 43292.6 \pm 23287.9 \text{ km}$ $e = 0.15 \pm 1.59$ $i = 0.83 \pm 9.13 \text{ deg}$ RMS = 1.0 arcs
<i>Case 4</i> – Gibraltar – Zimmerwald – 3 obs. from each station – 15 minute arc	$a = 42147.7 \pm 38.3 \text{ km}$ $e = 0.0258 \pm 0.0133$ $i = 0.1513 \pm 0.0809 \text{ deg}$ RMS = 0.28 arcs

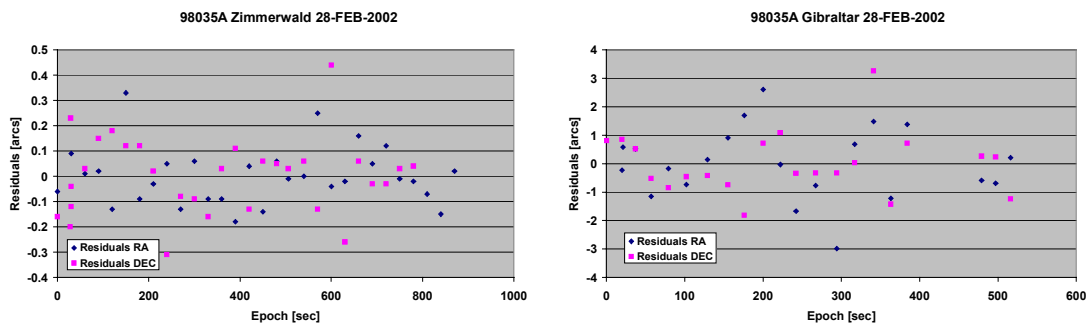


Fig. 12. Post-fit residuals (6-parameter orbit determination) for a single-site 8-minute arc of observations from Zimmerwald (left) and for a 15-minute arc of observations from Gibraltar (right).

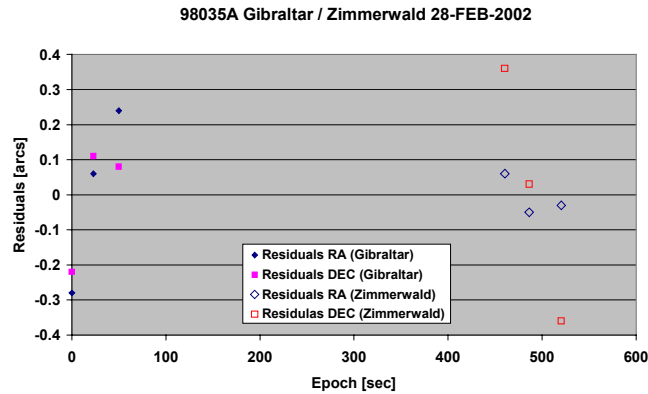


Fig. 13. Post-fit residuals (6-parameter orbit determination) for a 15-minute arc of observations from Zimmerwald and Gibraltar.

## 5. CONCLUSIONS

ESA has been conducting several GEO survey campaigns using its 1-meter telescope on Tenerife. Observations from the ESA telescope substantially contributed to the IADC sponsored GEO survey campaigns.

The results from the IADC spring 2002 campaign confirm the findings from the much longer ESA campaign in 2001.

The absolute magnitude distribution of the observed objects is bimodal with a prominent concentration of catalogued objects at the expected magnitude of about 12.5 and a large population of unknown objects fainter than about magnitude 15. The cutoff in number of objects fainter than about magnitude 19 – corresponding to an object size of about 15 centimeters – is entirely due to the sensitivity limit of the observation system. The real population of unknown small objects could therefore still increase beyond magnitude 19.

Several clusters of small objects sharing similar dynamical characteristics have been found. The only reasonable explanation for the origin of these clusters are explosions.

The short arcs of angle-only data acquired during typical surveys prevent the determination of elliptical orbits. For objects with considerably eccentric orbits like GTOs the assumption of circular orbits will mimic a dynamically totally different population compared to the real one.

Simultaneous multi-site observations may be used to overcome the orbit determination problem. A multi-site trial observing campaign was carried out to demonstrate feasibility of the method.

## 6. ACKNOWLEDGEMENTS

Part of this work was done under ESA/ESOC contract 11914/96/D/IM. The Gibraltar observations were carried out by Observatory Sciences Ltd. under contract from the UK Ministry of Defense.

## 7. REFERENCES

1. Africano, J.L. and Schildknecht, T., “International Geostationary Observation Campaign”, IADC A112.1 Report, September 2000.
2. Africano, J.L. et al., “A Geosynchronous Orbit (GEO) Search Strategy”, in these proceedings.
3. Dick, J.S.B., Herridge, P.S.C., Schildknecht, T., Ploner, M., Bain, M., Holland, D., “A Experimental European Multi-Site Deep-Space Optical Campaign”, 20<sup>th</sup> IADC Meeting, 8-12 April 2002, Guildford UK.
4. Wegener, P., Bendisch, J., Wiedemann, C., “The Reference Population of the MASTER 2001 Model”, 52<sup>nd</sup> IAF Congress, Toulouse, France, October 1-5, 2001.
5. Schildknecht, T., Ploner, M. and Hugentobler, U., “The Search for Debris in GEO”, 33<sup>rd</sup> COSPAR Scientific Assembly, July 16 – 23, 2000, Warsaw, Poland, Adv. in Space Research, Vol. 28, No. 9, pp. 1291-1299, 2001.
6. Schildknecht, T., Musci, R., Ploner, M., Preisig, S., de Leon Cruz, J., and Krag, H., “Optical Observation of Space Debris in the Geostationary Ring”, 3<sup>rd</sup> European Conference on Space Debris, 19 – 21 March 2001, ESOC, Darmstadt, Germany.